structure is measured to have a 32-GHz frequency response and withstands at least 32 mA photocurrents.

This result pushes the state of the art, even for surface-illuminated *p*-i-n photodiodes. Williams et al.[4] predict maximum detector photocurrents of 100 mA should be possible for well-designed 20-GHz devices; although the largest reported DC photocurrent is 40 mA for an 11-GHz device.[5]

The detector responsivity, saturation, and nonlinearity are examined. The measured DC responsivity, $\mathfrak{R}$, is approximately 0.45 A/W for both waveguide structures. The nonlinearity of the waveguide detectors are investigated at the second-harmonic frequency. The second-order intercept point (IP2) is extrapolated from the measured second harmonics to +34.5 dBm (output referenced) for the FKE waveguide detector and +32.6 dBm for the four-layer structure.

*Fermionics Corp., 4555 Runway Dr., Simi Valley, California 93063
**NCCOSC RDTE DIV 895, San Diego, California 92152-5000

1. M.C. Wu, L.Y. Lin, T. Itoh, T. Vang, in *Sixth Annual ARPA Symposium on Photonic Systems for Antenna Applications* (PSAA-6, 1996).
2. A.R. Williams, A.L. Kellner, P.K.L. Yu, Electron. Lett. **29**, 1298–1299 (1993).
3. R.B. Welstand, S.A. Pappert, C.K. Sun, J.T. Zhu, Y.Z. Liu, P.K.L. Yu, IEEE Photon. Technol. Lett. **8**, (November 1996).
4. K.J. Williams, R.D. Esman, M. Dagenais, IEEE J. Lightwave Technol. **14**, 84–96 (1996).
5. J. Paslaski, P.C. Chen, I.S. Chen, N. Bar-Chaim, in *Optical Fiber Communication Conference*, Vol. 4, 1994 OSA Technical Digest Series (Optical Society of America, Washington, D.C., 1994).

TuI6 3:15pm

Figure of merit for high-power, high-speed photodetectors

L.Y. Lin, M.C. Wu, T. Itoh, *Electrical Engineering Department UCLA, 66-147D Engineering IV, Los Angeles, California 90095-1594; E-mail: wu@ee.ucla.edu*

High-power, high-speed photodetectors are the key components for analog-fiber-optic links, which have applications in antenna remoting, CATV distribution, and wireless networks with fiber backbones. Photodetectors with high saturation power can greatly increase the RF link gain, signal-to-noise ratio, and spurious-free dynamic range (SFDR). Previously, we have proposed and experimentally demonstrated a velocity-matched distributed photodetector (VMDP) which can dramatically increase the saturation photocurrent without sacrificing its bandwidth. A very high saturation photocurrent of 56 mA and a 3-dB bandwidth of 49 GHz have been achieved.[1]

Though the trade-off between bandwidth and quantum efficiency has been analyzed for conventional high speed photodetectors,[2], optimization of photodetectors for high saturation power requires completely different design philosophy. In this paper, we report on the fundamental analysis of the trade-offs between the maximum achievable saturation photocurrent (I_{SAT}) and the 3-dB bandwidth (f_{3dB}) of high-power, high-speed photodetectors. The experimental results of the VMDP are presented and compared with the theory. Figure 1 shows the schematic structures of (1) surface-illuminated photodetectors, (2) waveguide photodetectors (WGPD), (3) velocity-mismatched traveling-wave photodetectors (TWPD),[3] and (4) the VMDP. In contrast to the numerical analysis,[4] close-form expressions has been obtained for the maximum

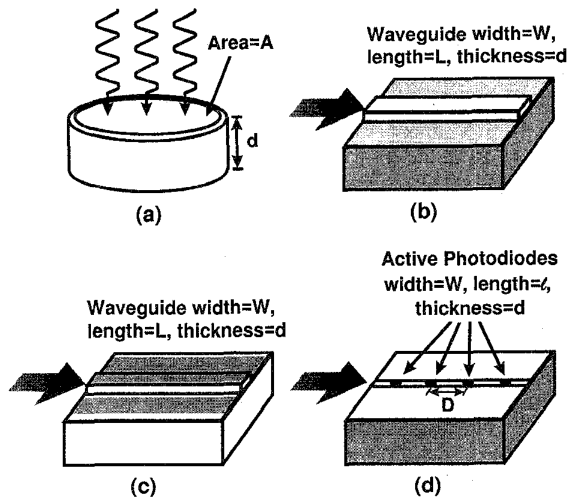

TuI6 Fig. 1. Schematic structures of: (a) surface-illuminated photodetectors; (b) waveguide photodetectors (WGPD); (c) velocity-mismatched traveling-wave photodetectors (TWPD); (d) velocity-matched distributed photodetectors (VMDP).

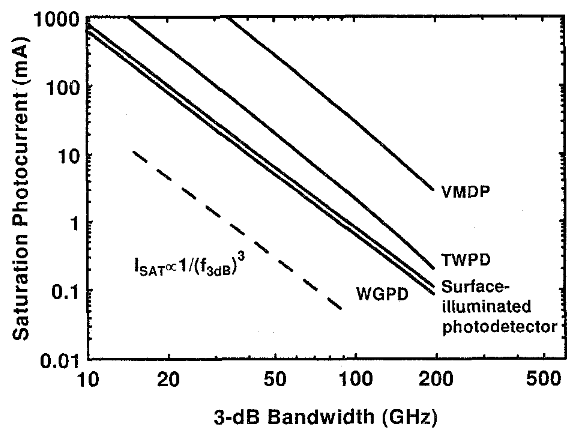

TuI6 Fig. 2. The trade-off between saturation photocurrent and 3-dB bandwidth for surface-illuminated photodetectors, waveguide photodetectors (WGPD), velocity-mismatched traveling-wave photodetectors (TWPD), and velocity-matched distributed photodetectors (VMDP).

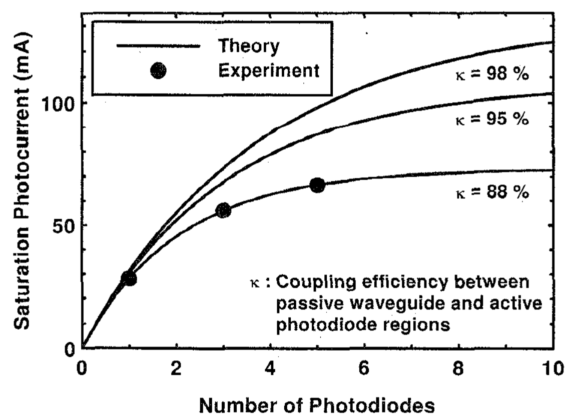

TuI6 Fig. 3. The theoretical and experimental AC saturation photocurrents of VMDP vs. the number of photodiodes for three coupling efficiency between passive waveguide and active photodiode regions: κ = 88%, 95%, and 98%.

saturation photocurrents. Figure 2 shows the maximum saturation photocurrent I_{SAT} versus f_{3dB} for the four different photodetector structures. The VMDP exhibits the highest saturation photocurrent because it can achieve large effective absorption volume without sacrificing its bandwidth or efficiency. Another interesting feature is that the I_{SAT} is inversely proportional to the cube of f_{3dB} for all photodetector structures. The figure of merit (FOM) can therefore be defined as $I_{SAT} \cdot (f_{3dB})^3$. The FOMs for the four photodetector structures are summarized in the following:

Surface-illuminated photodetector:

$$I_{SAT} \cdot (f_{3dB})^3 = \frac{I_S}{6\pi R_L \varepsilon}\left(\frac{V}{3.3}\right)^3 = 8.2 \times 10^5 (\mathrm{mA} \cdot \mathrm{GHz}^3)$$

$$\text{WGPD: } I_{SAT} \cdot (f_{3dB})^3 = \frac{I_S}{6\pi R_L \varepsilon}\left(\frac{V}{3.3}\right)^3 \frac{\eta}{-\ln(1-\eta)} = 6.4 \times 10^5 (\mathrm{mA} \cdot \mathrm{GHz}^3)$$

$$\text{TWPD: } I_{SAT} \cdot (f_{3dB})^3 = \frac{I_S}{6\pi R_{TWPD} \varepsilon}\left(\frac{V}{3.3}\right)^3 \left(\frac{\eta}{-\ln(1-2\eta)}\right)\left(1 - \frac{f_{3dB}}{f_{vm}}\right)^3 = 3.1 \times 10^6 \left(1 - \frac{f_{3dB}}{f_{vm}}\right)^3 (\mathrm{mA} \cdot \mathrm{GHz}^3)$$

$$\text{VMDP: } I_{SAT} \cdot (f_{3dB})^3 = \frac{I_S N}{6\pi R_{VMDP} \varepsilon}\left(\frac{V}{3.3}\right)^3 \frac{\eta}{-\ln(1-2\eta)} = 4.1 \times 10^7 (\mathrm{mA} \cdot \mathrm{GHz}^3)$$

where $I_S = 0.15\ \mathrm{mA}/\mu\mathrm{m}^3$ is the saturation photocurrent density,[4] V is the saturation velocity of the carriers ($= 8 \times 10^6$ cm/sec), R_L is the load resistance ($= 50\ \Omega$), f_{vm} is the 3-dB bandwidth limited by the velocity mismatch in TWPD, N is the number of active photodiodes in VMDP, and R_{TWPD} and R_{VMDP} are the contact resistances of TWPD and VMDP, respectively. The quantum efficiency is assumed to be 40% except for the surface-illuminated photodetectors. The details of the theoretical analysis will be reported at the conference.

As shown in Table 1, the VMDP has the highest FOM, followed by the TWPD. The WGPD has similar FOM as the surface-illuminated photodetectors, however, the quantum efficiency is higher for WGPD. Experimentally, the saturation photocurrents of the VMDP with various number of active photodiodes are measured and compared with the theoretical simulation. The results are shown in Fig. 3. Saturation photocurrent of 56 mA has been achieved for VMDPs with 49-GHz bandwidth. Theoretical calculation shows that saturation photocurrent greater than 100 mA can be achieved.

In summary, we have reported the theoretical analysis and proposed the FOM for high-power, high-speed photodetectors. The theoretical and experimental results show that the VMDP can achieve high saturation power and broad bandwidth.

1. L.Y. Lin, M.C. Wu, T. Itoh, T.A. Vang, R.E. Muller, D.L. Sivco, A.Y. Cho, IEEE Photon. Technol. Lett. **8**, (1996).
2. J.E. Bowers, C.A. Burrus, IEEE J. Lightwave Technol. **5**, 1339–1350 (1987).
3. K.S. Giboney, R.L. Nagarajan, T.E. Reynolds, S.T. Allen, R.P. Mirin, M.J.W. Rodwell, J.E. Bowers, IEEE Photon. Technol. Lett. **7**, 412–414 (1995).
4. K.J. Williams, R.D. Esman, M. Dagenais, IEEE J. Lightwave Technol. **14**, 84–96 (1996).

TuI7 3:30pm

Measurements of InGaAs metal-semiconductor-metal photodetector nonlinearities

Keith J. Williams, Ronald D. Esman, Steven Williamson,* Janis Valdmanis,* *Naval Research Laboratory, Code 5670, Washington, D.C. 20375; E-mail: keith.williams@nrl.navy.mil*

The use of 200-mW low-noise lasers in externally modulated fiber-optic links can increase the link dynamic range and reduce the noise figure by 10 dB per current decade above 1 mA. To realize this, these systems require high-speed photodetectors (PDs) capable of detecting up to 50 mA. To date, PDs capable of detecting this current level have been limited to frequencies below a few Gigahertz,[1] although 5–10 mA commercial 15–18 GHz devices are now available. Metal-semiconductor-metal (MSM) PDs offer possible optical power density and heat dissipation advantages over commercial *p*-i-n structures because the incident light can be spread over a larger surface area. These devices however, may be limited by space-charge effects[2–4] due to their less uniform absorbing region electric field. Here we present experimental nonlinearity (NL) results showing that these devices behave similarly to *p*-i-n devices when illuminated with high powers.

The PD under study has an undoped $In_{0.53}Ga_{0.47}As$ active-layer thickness of 0.5 μm. The interdigitated MSM electrodes are 1 μm in width and spacing. The diameter of the electrode pattern is 50 μm. The temporal response of the PD is 15 ps, which transforms to a 3-dB bandwidth (electrical power) of 21 GHz. The device is front-side illuminated via a 50 μm core multimode fiber yielding a responsivity of 0.25 A/W at 1.319 μm.

Significant insight into PD nonlinear behavior is obtained with a NL measurement versus electric field strength. The measurement system[4] used for this measurement consists of two equal-power 1.319-μm Nd:YAG lasers offset phase locked at 5 GHz. To characterize PD NL versus absorbing region electric field strength, the incident average optical power is held constant and the PD applied reverse bias voltage is adjusted. The resulting fundamental and harmonics are plotted in Fig. 1. For low voltages (0 to −4 V), the NL output increases and then peaks when the fundamental power is within a few dB of its value at high applied voltages. At higher applied biases (−4 to −6 V), the NL output generally decreases until −6 V, when the harmonic distortion is nearly independent of bias voltage. At −10 V, the second and third harmonics of this device are −54 and −62 dBc, respectively. This is compared to previous second- and third-harmonic measurements[4] of three *p*-i-n devices ranging between −53 to −63 dBc and −72 to −83 dBc, respectively.

The harmonic growth rate with PD current is shown in Fig. 2. As can be seen, the PD NL exhibits less than power law growth, with the second harmonic showing a local minimum near 1.8 mA. This minimum is due to the transition from an electron-velocity-dominant NL regime to a regime of constant NL level (constant with increasing bias). This was verified by repeating the measurements displayed in Fig. 1 (1mA) at 2 mA, where the transition from a decreasing to level NL increased from